Biogeosciences

Long-term spatial and temporal variation of CO_2 partial pressure in the Yellow River, China

L. Ran[1], **X. X. Lu**[1,2], **J. E. Richey**[3], **H. Sun**[4], **J. Han**[4], **R. Yu**[2], **S. Liao**[5], and **Q. Yi**[6]

[1]Department of Geography, National University of Singapore, 117570, Singapore
[2]College of Environment & Resources, Inner Mongolia University, Hohhot, 010021, China
[3]School of Oceanography, University of Washington, Box 355351, Seattle, WA 98195-5351, USA
[4]Institute of Geology and Geophysics, Chinese Academy of Sciences, Beijing, 100029, China
[5]Tongguan Hydrographic Station, Yellow River Conservancy Commission, Tongguan, 714399, China
[6]Toudaoguai Hydrographic Station, Yellow River Conservancy Commission, Baotou, 014014, China

Correspondence to: X. X. Lu (geoluxx@nus.edu.sg)

Abstract. Carbon transport in river systems is an important component of the global carbon cycle. Most rivers of the world act as atmospheric CO_2 sources due to high riverine CO_2 partial pressure (pCO_2). By determining the pCO_2 from alkalinity and pH, we investigated its spatial and temporal variation in the Yellow River watershed using historical water chemistry records (1950s–1984) and recent sampling along the mainstem (2011–2012). Except the headwater region where the pCO_2 was lower than the atmospheric equilibrium (i.e. 380 µatm), river waters in the remaining watershed were supersaturated with CO_2. The average pCO_2 for the watershed was estimated at 2810 ± 1985 µatm, which is 7-fold the atmospheric equilibrium. As a result of severe soil erosion and dry climate, waters from the Loess Plateau in the middle reaches had higher pCO_2 than that from the upper and lower reaches. From a seasonal perspective, the pCO_2 varied from about 200 µatm to $> 30\,000$ µatm with higher pCO_2 usually occurring in the dry season and lower pCO_2 in the wet season (at 73 % of the sampling sites), suggesting the dilution effect of water. While the pCO_2 responded exponentially to total suspended solids (TSS) export when the TSS concentration was less than $100\,\mathrm{kg\,m^{-3}}$, it decreased slightly and remained stable if the TSS concentration exceeded $100\,\mathrm{kg\,m^{-3}}$. This stable pCO_2 is largely due to gully erosion that mobilizes subsoils characterized by low organic carbon for decomposition. In addition, human activities have changed the pCO_2 dynamics. Particularly, flow regulation by dams can diversely affect the temporal changes of pCO_2, depending on the physiochemical properties of the regulated waters and adopted operation scheme. Given the high pCO_2 in the Yellow River waters, large potential for CO_2 evasion is expected and warrants further investigation.

1 Introduction

Rivers play a crucial role in the global carbon cycle, because they can modulate the carbon dynamics not only of the watersheds but also of the coastal systems into which river waters are discharged (Aufdenkampe et al., 2011). Fluvial carbon export represents an important pathway linking land and the ocean. Approximately 0.9 Gt of carbon is delivered into the oceans per year via inland waters (Cole et al., 2007; Battin et al., 2009). However, rivers are not merely passive conduits. Evidence is accruing to indicate that, while only a small portion of carbon that enters a river network finally reaches the ocean, a considerable fraction would be buried within the river network or returned to the atmosphere en route (Yao et al., 2007; Wallin et al., 2013). Consequently, rivers are viewed as sources of atmospheric carbon dioxide (CO_2) (Cole et al., 2007; Butman and Raymond, 2011). Recent estimates show that global inland waters can transfer 0.75–$2.1\,\mathrm{Gt\,C\,yr^{-1}}$ into the atmosphere (Cole et al., 2007; Tranvik et al., 2009; Raymond et al., 2013). Comparative studies associated with lateral carbon fluxes have highlighted the significance of CO_2 evasion in assessing global carbon
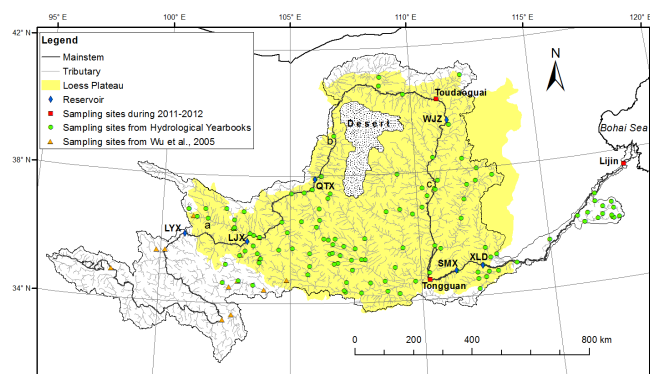
Figure 1. Location map of the sampling sites in the Yellow River watershed. Acronyms for the mainstem dams: LYX – Longyangxia since 1986; LJX – Liujiaxia since 1968; QTX – Qingtongxia since 1968; WJZ – Wanjiazhai since 1998; SMX – Sanmenxia since 1960; and XLD – Xiaolangdi since 2000.

budget (Melack, 2011). For example, Richey et al. (2002) show that CO_2 emission in the Amazon River basin is an order of magnitude greater than fluvial export of organic carbon to the ocean.

Decomposition of terrestrially derived organic carbon and aquatic respiration are the primary sources of riverine CO_2 (Humborg et al., 2010). As an important parameter in estimating CO_2 outgassing, partial pressure of riverine CO_2 (pCO_2) indicates the CO_2 concentration in rivers and the gradient relative to the atmospheric equilibrium (i.e. 380 µatm). Most rivers of the world have higher pCO_2 than the overlying atmosphere, suggesting a great emission potential (Cole et al., 2007; Striegl et al., 2012). While the riverine pCO_2 of mainstem or estuary waters has been widely recognized, such as the Amazon (Richey et al., 2002), Pearl (Yao et al., 2007), and Columbia (Evans et al., 2013), a holistic assessment concerning a complete river network is rare. This is largely caused by the constraints of time and logistics to conduct spatial sampling covering not only the mainstem but also the lower stream-order tributaries. Indeed, tributaries are physically and biogeochemically more active because they have stronger turbulence and more rapid mixing with the benthic substrate and the atmosphere than the mainstem (Alin et al., 2011; Butman and Raymond, 2011; Benstead and Leigh, 2012). For instance, Aufdenkampe et al. (2011) found that the CO_2 outgassing fluxes from small streams could be 2–3 times higher than from larger rivers. Thus, estimating CO_2 evasion based only on mainstem waters will underestimate the total efflux of a specific river system. Analysing pCO_2 at space- and timescales by high-resolution sampling is a prerequisite for precisely evaluating CO_2 outgassing and its implications for the carbon cycle.

The Yellow River is characterized by high sediment and total dissolved solids (TDS) among the world's large rivers, primarily because of severe soil erosion and intensive chemical weathering and human activity. Its TDS concentration

of 452 mg L^{-1} is about four times the world median value (Chen et al., 2005). Based on measurements at hydrological gauges or in specific river reaches, prior studies have investigated its chemical weathering and carbon transport (e.g. Zhang et al., 1995; Wu et al., 2008; Wang et al., 2012; Ran et al., 2013). Soil respiration in terrestrial ecosystems and impact of land use change on carbon storage have also been analysed (Zhao et al., 2008; Li et al., 2010). By contrast, few studies have examined its carbon dynamics in river waters and how riverine pCO_2 has responded to catchment features (Wang et al., 2012; Ran et al., 2013). Using historical records across the watershed during the period 1950s–1984 and recent sampling along the mainstem, we calculated the riverine pCO_2 from alkalinity and pH. This study aimed to investigate the spatial and temporal variation of pCO_2 and its responses to natural and human factors. The results will provide insights into the coupling between soil erosion and riverine pCO_2 and the impact of dam operation on downstream riverine pCO_2 changes.

2   Materials and methods

2.1   The Yellow River

The Yellow River drains 752 000 km^2 of north China, originating in the Tibetan Plateau and flowing eastward into the Bohai Sea (Fig. 1). Located in a semiarid–arid climate, its precipitation is spatially highly variable, decreasing from 700 mm yr^{-1} in the southeast to 250 mm yr^{-1} in the northwest (Zhao, 1996). Likewise, temperature changes significantly, with the mean temperature in the upper (above Toudaoguai), middle (approximately between Toudaoguai and the Xiaolangdi Dam), and lower (below the Xiaolangdi Dam) reaches being 1–8, 8–14 and 12–14 °C, respectively (Chen et al., 2005). Because the Yellow River basin is in large part surrounded by the Loess Plateau that has typically accumulated huge erodible loess deposits (Fig. 1), it suffers from severe soil erosion. Approximately 1.6 Gt of sediment was transported to the ocean per year prior to the 1970s (Syvitski et al., 2005). For comparison, the mean water discharge was only 49 km^3 yr^{-1} over the same period (Zhao, 1996).

Both hydrological regime and landscape within the watershed have been greatly altered due to intensive human activity (Ran and Lu, 2012). While the water discharge has dropped to 15 km^3 yr^{-1} during the recent decade, the sediment flux has decreased to about 0.14 Gt yr^{-1} as a result of massive soil conservation and sediment trapping by dams. Among the numerous dams, these constructed on the mainstem channel play fundamental roles in regulating delivery of water, sediment and dissolved solids (Ran and Lu, 2012), especially the joint operation of the Sanmenxia and Xiaolangdi dams since 2000. With about 140 million people currently residing within the watershed, the population density is 180 person km^{-2} (Chen et al., 2005), and it exceeds

Table 1. pH at Luokou station during the period 1980–1984: a comparison of different data sources (arithmetic mean ± standard deviation).

	Year				
Data source	1980	1981	1982	1983	1984
GEMS/Water Programme	8.27 ± 0.11	8.21 ± 0.21	8.10 ± 0.20	8.14 ± 0.10	8.25 ± 0.09
This study	8.11 ± 0.13	8.14 ± 0.07	8.13 ± 0.07	8.10 ± 0.03	8.09 ± 0.05
% of variation	1.93	0.85	−0.37	0.49	1.94

300 person km^{-2} in some agricultural areas in the middle reaches. Consequently, land use has become increasingly both extensive and intensive.

The Yellow River basin was mainly developed on the Sino-Korean Shield with Quaternary loess deposits overlying the vast middle reaches and Archean to Tertiary granites and metamorphic rocks in areas near the basin boundaries and in the lower reaches (Chen et al., 2005). Chemical analyses of loess samples show that feldspar, micas and quartz are the most common detrital minerals with carbonates accounting for 10–20 % (Zhang et al., 1995). Because the loess deposits cover about 46 % of the total drainage area, the river presents high alkalinity and intense rock weathering. With exceptionally high TDS concentration the Yellow River delivers around 11 Mt of dissolved solids per year to the Bohai Sea (Gaillardet et al., 1999).

2.2 Historical records of water chemistry

Historical records of major ions (e.g. Ca^{2+}, Mg^{2+}, Na$^+$, K$^+$, Cl$^-$, HCO$_3^-$ and SO$_4^{2-}$) measured from a hydrological monitoring network were extracted from the Yellow River Hydrological Yearbooks, which are yearly produced by the Yellow River Conservancy Commission (YRCC). Other variables concurrently measured at each sampling event, including pH, water temperature, water discharge and total suspended solids (TSS), were also retrieved from the yearbooks for this study. The water samples for pH and temperature were taken in the same time period as these for ion analysis. Over the period from the 1950s to 1984, the sampling frequency ranged from 1 to 5 times per month, depending on hydrological regime. Sampling at some stations during the period 1966–1975 were suspended or completely stopped. Post-1984 records are not in the public domain. Given the discontinuity in sampling, only the stations with at least 6 samples in a year were analysed. A total of 129 stations with 15 029 water chemistry measurements were compiled (Fig. 1).

Chemical analyses of the collected water samples were performed under the authority of the YRCC following the standard procedures and methods described by Alekin et al. (1973) and the American Public Health Association (1985). The pH and temperature were measured in field, and total alkalinity (TAlk) was determined using a fixed end-point titration method. Detailed description of the sampling

and analysis procedures can be found in Chen et al. (2002a). The results are summarized in the Supplement (Table S1).

Use of historical records always raises the issue of data reliability. No detailed information on quality assurance and quality control is available in the hydrological reports. Extensive efforts have been made to assess the data quality by analysing the parameter differences measured at the same station but by different agencies. The Luokou station on the lower Yellow River mainstem has been monitored under the United Nations Global Environment Monitoring System (GEMS) Water Programme since 1980 (only yearly means available at http://www.unep.org/gemswater). As pCO$_2$ is considerably sensitive to pH changes (Li et al., 2012), the pH values from the two sources were compared (Table 1), which showed that the data set from the Hydrological Yearbooks agreed well with the GEMS/Water Programme data set with differences of < 2 %. High data quality of the hydrological reports can also be confirmed from the concentration comparison of major ions in the two data sets (see Chen et al., 2005).

Given the data paucity for the upper Yellow River, data collected at 17 sites in the headwater region were retrieved from Wu et al. (2005) (Fig. 1 and Table S1 in the Supplement). They measured pH and temperature along the mainstem and major tributaries and determined the TAlk through Gran titration. Comparison with previous sampling results (Zhang et al., 1995) showed their data agreed well.
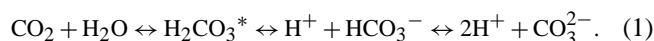
2.3 Recent field sampling

From July 2011 to July 2012, weekly sampling on the mainstem was undertaken at Toudaoguai, Tongguan and Lijin stations (Fig. 1). The frequency increased (i.e. daily) when large floods occurred. Water column samples were collected ∼ 0.5 m below the surface water and kept in acid-washed, but carefully neutralized, high-density polyethylene containers. Concomitant determination of pH and water temperature was performed in situ using a Hanna HI9125 pH meter on the NBS scale, which was calibrated prior to each measurement against pH7.01 and pH10.01 buffers. Replicate measurements showed the precision for pH and temperature were ±0.04 units and ±0.1 °C, respectively. The TAlk was determined by titrating 50 mL filtered water through 47 mm Whatman GF/F filters (0.7 μm pore size) with 0.02 M HCl solution within 5 h after sampling. Three parallel titrations showed

the analytical error was below 3 %. The parallel alkalinity results were then averaged. In total, 163 samples were collected. Ancillary data, including daily water discharge and TSS, were acquired from the YRCC. Generally, the sampling results at Toudaoguai and Tongguan reflect the TAlk and pCO$_2$ changes on the Loess Plateau, while the Lijin measurements represent seaward export as it is located 110 km upstream of the river mouth and free of tidal influences.

2.4 Calculations of DIC species and pCO$_2$

Total dissolved inorganic carbon (DIC) species in river systems include HCO$_3^-$, CO$_3^{2-}$, H$_2$CO$_3$ and aqueous CO$_2$ (CO$_{2aq}$). Their relative concentration is a function of temperature and pH (Li et al., 2012). DIC species can be determined by Henry's Law, from which the pCO$_2$ can be calculated using the CO2SYS program (Lewis and Wallace, 1998):

$$\text{CO}_2 + \text{H}_2\text{O} \leftrightarrow \text{H}_2\text{CO}_3{}^* \leftrightarrow \text{H}^+ + \text{HCO}_3{}^- \leftrightarrow 2\text{H}^+ + \text{CO}_3^{2-}. \quad (1)$$

At chemical equilibrium, the activities of the reactants and products are determined from the thermodynamic reaction constants (K_i) that are temperature (T) dependent:

$$K_{\text{CO}_2} = [\text{H}_2\text{CO}_3{}^*]/[p\text{CO}_2] \quad (2)$$

$$K_1 = [\text{H}^+][\text{HCO}_3{}^-]/[\text{H}_2\text{CO}_3{}^*] \quad (3)$$

$$K_2 = [\text{H}^+][\text{CO}_3{}^{2-}]/[\text{HCO}_3{}^-], \quad (4)$$

where H$_2$CO$_3^*$ is the sum of CO$_{2aq}$ and the true H$_2$CO$_3$. The pK_i values (negative log of K_i) can be calculated by the following equations (Clark and Fritz, 1997):

$$pK_{\text{CO}_2} = -7 \times 10^{-5} T^2 + 0.016T + 1.11 \quad (5)$$

$$pK_1 = 1.1 \times 10^{-4} T^2 - 0.012T + 6.58 \quad (6)$$

$$pK_2 = 9 \times 10^{-5} T^2 - 0.0137T + 10.62 \quad (7)$$

Then, the pCO$_2$ can be simply expressed as:

$$p\text{CO}_2 = [\text{H}_2\text{CO}_3{}^*]/K_{\text{CO}_2} = [\text{H}^+][\text{HCO}_3{}^-]/K_{\text{CO}_2}K_1. \quad (8)$$

With the pH mostly ranging from 7.4 to 8.6 indicative of natural processes for the Yellow River (Chen et al., 2005), HCO$_3^-$ is considered equivalent to alkalinity because it represents > 96 % of the TAlk. This approach has been frequently used and has demonstrated high pCO$_2$ in Chinese river systems (e.g. Yao et al., 2007; Li et al., 2012). To validate the simplification, we also estimated the pCO$_2$ using the program PHREEQC (Hunt et al., 2011). The pCO$_2$ result derived by PHREEQC are very close to that by CO2SYS with < 3 % differences. However, the calculated pCO$_2$ results may have slightly overestimated the actual values (Cole and Caraco, 1998; Abril et al., 2015).
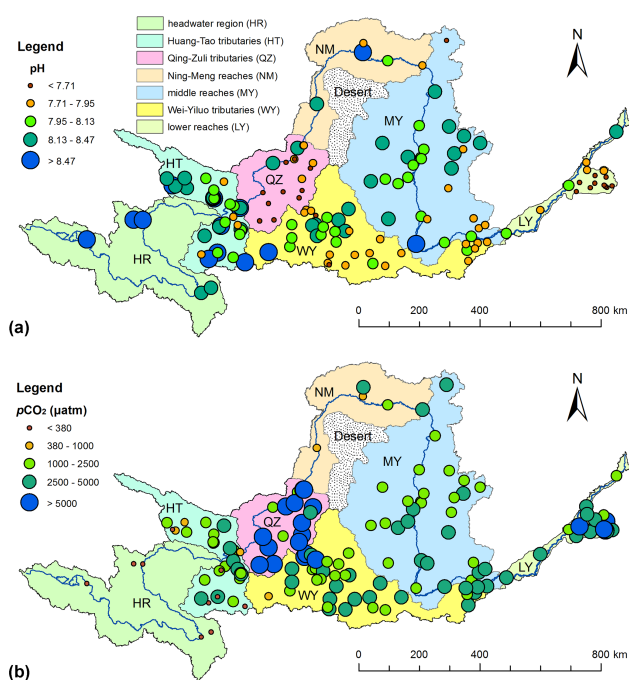

Figure 2. Spatial variations of pH **(a)** and pCO$_2$ **(b)** in the Yellow River watershed.

3 Results

3.1 Characteristics of hydrochemical setting

To better investigate the spatial changes of hydrochemical variables, the watershed was divided into seven sub-basins: the headwater region (HR), the Huang–Tao tributaries (HT), the Qing–Zuli tributaries (QZ), the Ning–Meng reaches (NM), the Wei–Yiluo tributaries (WY), the middle reaches (MY), and the lower reaches (LY) (Fig. 2). The Yellow River waters were characterized by high alkalinity with the pH presenting significant spatial variations (Fig. 2a). While high pH values were mostly observed in the HR sub-basin where the highest was 9.1, relatively low pH (i.e. < 7.71) was recorded at the QZ tributary sites with the lowest being 6.4. For the waters from the Loess Plateau, the pH ranged from 7.71 to 8.47. Towards the river mouth, it showed a downward trend in the lower reaches (LY). With one exception at Lijin (Fig. 1), the pH values were all below 8.13 and even below 7 at some tributary sites. In addition to spatial variations, it showed considerable seasonal changes. As exemplified in Fig. 3a, the waters were generally more alkaline in the dry season (October–May) than in the wet season (June–September).

Similarly, with a range of 855–8633 µmol L^{-1}, the TAlk presented complex spatial variability throughout the watershed. While the HR and LY sub-basins showed the lowest TAlk (< 2600 µmol L^{-1}), the sub-basins on the Loess Plateau had considerably high alkalinity with a mean TAlk of
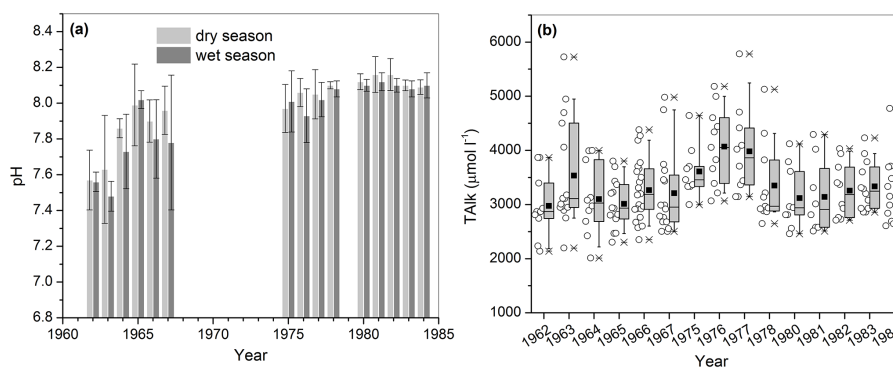
Figure 3. Seasonal comparison of pH (**a**) and box-and-whisker plot of TAlk (**b**) at Luokou station. The horizontal line is the median value, the black square is the mean value, the boxes represent the 25th to 75th percentile, the whiskers represent the 10th and 90th percentile, and the asterisks represent the maximum and minimum. Raw TAlk data are added to the left in (**b**).

$3850 \pm 1000\,\mu\mathrm{mol\,L}^{-1}$. The highest TAlk ($8633\,\mu\mathrm{mol\,L}^{-1}$) was measured in the QZ sub-basin. It is evident that the TAlk and pH showed similar spatial variations, but in the reverse direction with high TAlk coinciding with low pH (Fig. S1). With regard to all the sampling results, about 58 % of the TAlk values fell into the range of 3000–4000 $\mu\mathrm{mol\,L}^{-1}$ and 92 % into the range of 2000–5000 $\mu\mathrm{mol\,L}^{-1}$. For the whole Yellow River watershed, its mean TAlk was $3665 \pm 988\,\mu\mathrm{mol\,L}^{-1}$. In addition, its TAlk remained largely stable during the sampling period. Figure 3b shows an example of the TAlk changes at Luokou. Despite the discontinuous measurement from 1968 to 1974, the TAlk did not change significantly over time ($p = 0.48$).

3.2 Spatial and temporal variability of $p\mathrm{CO_2}$

The $p\mathrm{CO_2}$ varied significantly throughout the watershed with 2 orders of magnitude from $\sim 200\,\mu\mathrm{atm}$ to more than $30\,000\,\mu\mathrm{atm}$. Except the headwater region that showed lower $p\mathrm{CO_2}$ than the overlying atmosphere, the remaining watershed had a considerably high $p\mathrm{CO_2}$ (Fig. 2b). The highest $p\mathrm{CO_2}$ of $36\,790\,\mu\mathrm{atm}$ was estimated on a tributary in the QZ sub-basin resulting from low pH and high TAlk. For the middle Yellow River, including the MY and WY sub-basins, the waters were considerably supersaturated in $\mathrm{CO_2}$ with the $p\mathrm{CO_2}$ ranging from 1000 to 5000 $\mu\mathrm{atm}$ (Fig. 2b). Moreover, the $p\mathrm{CO_2}$ level in the lower Yellow River reaches (LY) was much higher and can exceed $10\,000\,\mu\mathrm{atm}$. On average, the $p\mathrm{CO_2}$ in the Yellow River watershed was $2810 \pm 1985\,\mu\mathrm{atm}$, 7-fold the atmospheric $\mathrm{CO_2}$ equilibrium. However, it must be recognized that, unlike the historical data set that was monthly measured, sampling in the HR sub-basin by Wu et al. (2005) was conducted only during the late May and June of 1999 and 2000 when the wet season had barely started. Given the flushing effect of infiltrating rainfall and snowmelt flows at the beginning of the wet season (Clow and Drever, 1996; Melack, 2011), the resultant TAlk and $p\mathrm{CO_2}$ are expected to be close to highest.

Similar to TAlk, the $p\mathrm{CO_2}$ at most sites also presented strong seasonal variations. At 73 % of the sampling sites, higher $p\mathrm{CO_2}$ occurred in the months before the onset of the wet season. During the wet season, it decreased to a relatively low level before going up from October onwards. The seasonal ratio of $p\mathrm{CO_2}$, defined as the ratio of $p\mathrm{CO_2}$ in the dry season over that in the wet season, ranged from 0.8 to 2.3. To more clearly show its spatial and temporal changes, Fig. 4 shows the high temporal-resolution results at Toudaoguai, Tongguan and Lijin. Both the TAlk and $p\mathrm{CO_2}$ exhibited large spatial differences among the three sites. The mean TAlk at Tongguan ($4075 \pm 796\,\mu\mathrm{mol\,L}^{-1}$) was higher than at the upstream Toudaoguai and the downstream Lijin (3664 ± 399 and $3622 \pm 292\,\mu\mathrm{mol\,L}^{-1}$, respectively). Likewise, the mean $p\mathrm{CO_2}$ at Tongguan ($4770 \pm 3470\,\mu\mathrm{atm}$) was about 3 and 3.5 times that at Toudaoguai ($1624 \pm 778\,\mu\mathrm{atm}$) and Lijin ($1348 \pm 689\,\mu\mathrm{atm}$), respectively. The highest $p\mathrm{CO_2}$ of $26\,318\,\mu\mathrm{atm}$ was estimated at Tongguan in early May.

Compared with tributary streams showing pronounced seasonal variation, the mainstem exhibited more complicated seasonal patterns (Fig. 4). The TAlk was higher in the dry season than in the wet season, in particular for Tongguan located downstream of the Loess Plateau (Table 2; Fig. 1). The $p\mathrm{CO_2}$ showed similar seasonal cycles. A contrast to the weak seasonal changes at Toudaoguai and Lijin, the $p\mathrm{CO_2}$ at Tongguan in the dry season ($6016\,\mu\mathrm{atm}$ on average) was twofold that in the wet season. It is clear the $p\mathrm{CO_2}$ increased substantially in both seasons as waters from the Loess Plateau entered the mainstem, and then decreased along the channel course towards the ocean (Table 2). Furthermore, the $p\mathrm{CO_2}$ presented complex relationships with water discharge. While the $p\mathrm{CO_2}$ changed synchronously with water at Toudaoguai, it decreased with increasing water in the wet season at Tongguan and Lijin (Fig. 4). The $p\mathrm{CO_2}$ at all three stations was significantly higher than the atmospheric equilibrium, though the gradient varied substantially between different stations or different seasons.
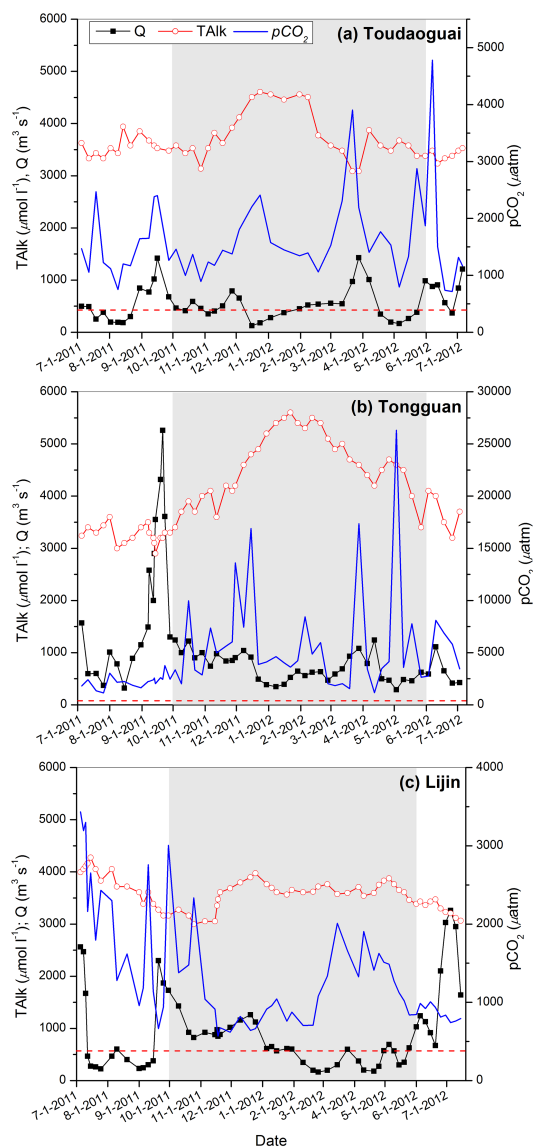
Figure 4. Weekly variations in water discharge (Q), TAlk, and pCO$_2$ at **(a)** Toudaoguai, **(b)** Tongguan and **(c)** Lijin from July 2011 to July 2012. The dotted line denotes the atmospheric CO$_2$ equilibrium (i.e. 380 µatm) and the shaded grey represents the dry season.
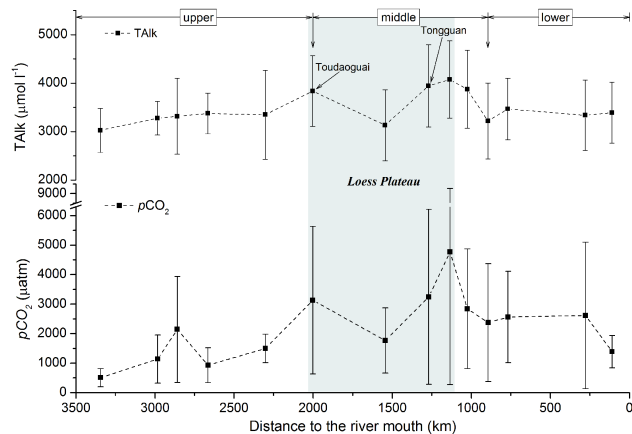

Figure 5. Longitudinal variations of TAlk and pCO$_2$ along the mainstem channel. The shaded region approximately represents the Loess Plateau. Whiskers indicate the standard deviation.

100 kg m^{-3}, however, the pCO$_2$ decreased slightly and remained stable thereafter (Fig. 6).

4   Discussion

4.1   Environmental controls on riverine pCO$_2$

The alkalinity of river water reveals its buffering capacity in a carbonate system to neutralize acids and bases. Due to abundant carbonate outcrops, groundwater in the Yellow River basin was highly alkaline (Chen et al., 2002b), which directly led to higher TAlk in the dry season when baseflow constituted 90 % of the river runoff. High TAlk on the Loess Plateau was probably the result of chemical weathering. With widespread carbonates, chemical weathering in the loess deposits has generated high dissolved solids with HCO$_3^-$ being the dominant ion (Zhang et al., 1995; Chen et al., 2005). Plotting TAlk against flow showed that they were negatively correlated (Fig. 7). However, the TAlk did not change synchronously with water in the wet season. It decreased more slowly as revealed by the exponents of the fitted equations. Compared with the flow changes, a narrower TAlk fluctuation suggested the coupling results of enhanced alkalinity export in the wet season and the dilution effect of water (Piñol and Avila, 1992; Raymond and Cole, 2003). Analysing the temporal variations of major ions during 1958–2000, Chen et al. (2005) found that they persistently increased due largely to human impacts. In contrast, the long-term stable TAlk (Fig. 3b) indicates that it is not significantly affected. Natural weathering processes must have played a more important role in controlling the export of DIC species and TAlk.

Carbon in river waters is largely derived from biogeochemical processes occurring in terrestrial ecosystems. Changes in terrestrial ecosystems will thus affect riverine carbon cycle. Because soil respiration and CO$_2$ production

Longitudinal variations of TAlk and pCO$_2$ along the mainstem indicated that the waters from the Loess Plateau had higher TAlk and were more supersaturated in CO$_2$ than the upper and lower Yellow River waters (Fig. 5). Both the TAlk and pCO$_2$ decreased remarkably downstream of the Loess Plateau. In addition, with extremely high suspended solids, the Yellow River provides an excellent case study for understanding the responses of pCO$_2$ to TSS export (Fig. 6). Based on measurements in the sediment-yielding areas on the Loess Plateau, the pCO$_2$ increased exponentially with increasing TSS concentration under low TSS scenarios (i.e. 100 kg m^{-3}). When the TSS concentration was higher than

Table 2. Inter-annual and seasonal differences of pH, TAlk, and pCO$_2$ at the three stations. The number below the station name denotes the channel length to the river mouth.

Station	Variable	1950s–1984		2011–2012	
		Wet season	Dry season	Wet season	Dry season
Toudaoguai	pH	7.89	8.01	8.19	8.11
(2002 km)	TAlk (µmol L^{-1})	3595	4091	3513	3771
	pCO$_2$ (µatm)	3716	2708	1580	1655
Tongguan	pH	–	–	7.91	7.72
(1147 km)	TAlk (µmol L^{-1})	–	–	3356	4562
	pCO$_2$ (µatm)	–	–	2927	6016
Lijin	pH	8.18	8.19	8.23	8.28
(110 km)	TAlk (µmol L^{-1})	2942	3789	3576	3584
	pCO$_2$ (µatm)	1344	1349	1609	1132
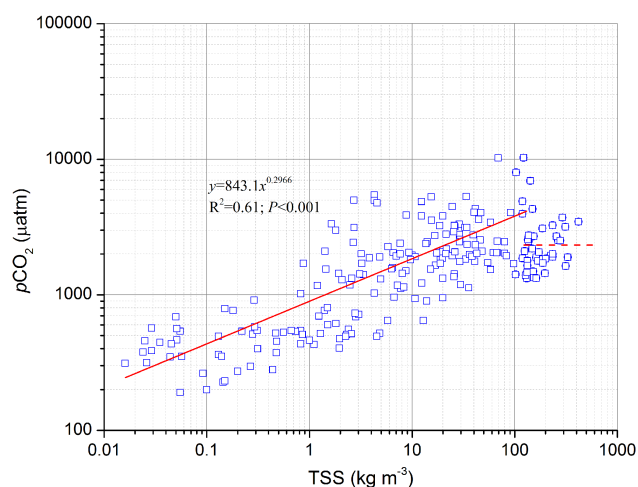
Figure 6. Relationship between total suspended solids (TSS) and pCO$_2$ based on measurements on the Loess Plateau. The solid line denotes the fitted line for the TSS concentration ranging from 0 to 100 kg m^{-3}, and the dashed line indicates the stable trend of pCO$_2$ when the TSS concentration is higher than 100 kg m^{-3}.

are highly dependent on temperature and rainfall (Epron et al., 1999; Hope et al., 2004; Shi et al., 2011), higher riverine pCO$_2$ is expected in the wet season due to soil CO$_2$ flushing. This is in contrast to the observed seasonal variations in the Yellow River. A unique precipitation distribution and hydrological regime may have contributed to these anomalous observations. The Yellow River basin is characteristic of high-intensity rainfalls; several storms in the wet season can account for > 70 % of the annual precipitation (Zhao, 1996). Coupled with its distinct soil surface microtopography with texture consisted mainly of silt and clay, Hortonian overland flow is the dominant runoff process (Liu and Singh, 2004). As a result of greatly reduced soil infiltration capacity, the generated overland flow by high-intensity rainfalls may have diluted the TAlk and caused the lowered riverine pCO$_2$.

Responses of the pCO$_2$ to TSS concentration (Fig. 6) reflect the soil erosion processes distinctive to the Loess Plateau (Zhao, 1996; Rustomji et al., 2008). At the initial stage of soil erosion, the surficial soils with abundant organic carbon are first eroded into river water. Decomposition of the labile organic carbon in the eroded soils will increase the pCO$_2$. Thus, it responded positively to soil erosion and TSS. This positive response lasted until the topsoils were completely eroded. The threshold of ca. 100 kg m^{-3} is consistent with the commonly defined hyperconcentrated flows (Xu, 2002). Hyperconcentrated flows indicating TSS concentration greater than 100 kg m^{-3} are frequently recorded in the Yellow River, in which gully erosion contributes > 50 % of the fluvial sediment loads (Ran et al., 2014). Compared with the organic carbon content in the topsoils (usually 0.5–1.5 %), it is much lower in the subsoils (i.e. 0.2–0.3 %) and shows uniformity with depth (Wang et al., 2010; Zhang et al., 2012). The mobilized subsoils through gully erosion therefore have lower organic carbon quantity for decomposition, resulting in the reduced and stable riverine pCO$_2$ regardless of the increasing TSS concentration.

Lower pCO$_2$ in the HR sub-basin was caused by relatively low TAlk and high pH. Statistical analyses showed that its TAlk was 25 % lower than the basin average while the pH was 7 % higher. Compared to other sub-basins, the HR sub-basin is covered by an alpine meadow ecosystem with soils being slightly eroded, which may have constrained the leaching of organic matter. Moreover, this sub-basin is in cold environments and its temperature falls below zero from October to March. Microbial decomposition of organic matter and ecosystem respiration are kinetically inhibited as affected by the low temperature (Kato et al., 2004), resulting in the low pCO$_2$. Unique climate also denotes the seasonal patterns of pCO$_2$ in the upper and middle Yellow River. Occurrence of the highest pCO$_2$ at Toudaoguai and Tongguan in March through May is likely controlled by ice-melt floods (Fig. 4a and b). In the coldest months, water surface
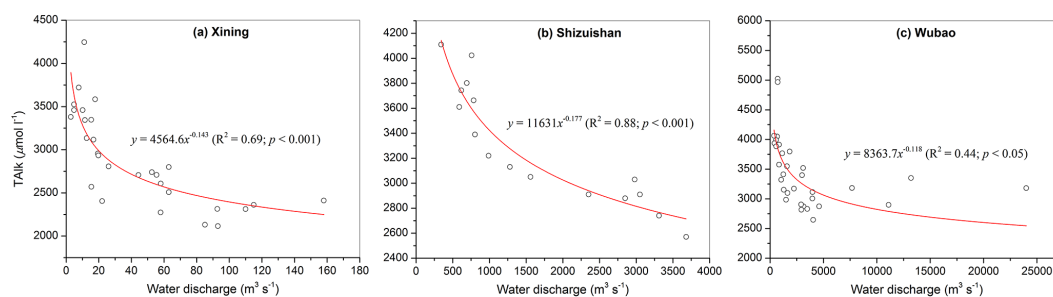
Figure 7. Dependence of TAlk on natural water discharge for different water discharge scales at typical sampling sites: **(a)** is from a tributary and **(b)** and **(c)** are from the Yellow River mainstem (see Fig. 1 for locations).
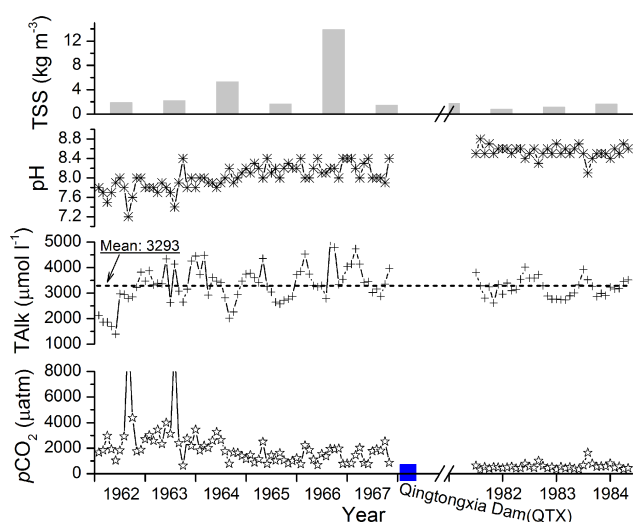

Figure 8. Impacts of Qingtongxia (QTX) dam on riverine TSS, pH, TAlk and pCO$_2$. Measurements were conducted ~ 850 m downstream of the dam that was built in 1968 (see Fig. 1 for its location).

in the northernmost reaches (between QTX and Toudaoguai; Fig. 1) will freeze up (Chen and Ji, 2005). Aqueous CO$_2$ could not be efficiently released due to ice protection and typically accumulates below the ice cover. Starting from early spring, the ice begins to thaw and CO$_2$-laden waters are exported downstream to the sampling sites, probably causing the sharply increased pCO$_2$. Also, the lower temperature in the dry season would be responsible for the higher pCO$_2$ as the solubility of CO$_2$ increases with decreasing water temperature.

High pCO$_2$ in the QZ sub-basin (Fig. 2b) was primarily the result of high TAlk due to its geological background. Its major rock types are carbonates, detritus (quartz and feldspar) and red-beds (gypsum and halite) (Zhang et al., 1995). These rocks are highly vulnerable to weathering, thus producing TAlk (mainly HCO$_3^-$) into river. In fact, its mean TDS was 8–14 times the basin average (Chen et al., 2005). Further, this sub-basin has high drought index with its annual evaporation being > 8 times the annual precipitation (Chen et

al., 2005). Such strong evaporation will result in not only the precipitation of minerals with low solubility, but also the elevated concentrations of solutes not removed during the crystallization process. Another possible cause is the severe erosion due to sparse vegetation cover. In addition to mobilization of organic matter, soil erosion is able to enhance chemical weathering by increasing the exposure surface of fresh minerals to atmosphere (Millot et al., 2002). This would also contribute to greatly condensed DIC species in river waters and thus high pCO$_2$.

As for the longitudinal variations (Fig. 5), severe soil erosion on the Loess Plateau may be the major reason as discussed above. In addition, low groundwater table in the arid climate allows deeper soil horizons to adequately interact with the atmosphere, which could also facilitate the exposure of mineral surfaces to weathering and generate huge quantities of alkalinity. Increasing pCO$_2$ until Tongguan suggested the integrated responses of pCO$_2$ to these factors. Without large tributaries joining the lower Yellow River (Fig. 1), the decreasing TAlk and pCO$_2$ along the mainstem revealed reduced TAlk input. Overall, the spatial changes of TAlk and pCO$_2$ were the combined results of differences in soil property, hydrological regime, climate and landform development.

4.2   Anthropogenic impacts on riverine pCO$_2$

Agricultural activity within a watershed can affect its riverine pCO$_2$. Tilling practices can not only expand the exposure area of soil materials, but also alter the hydrology of surficial soils, increasing the contact rate between water and minerals and thus the alkalinity export (Raymond and Cole, 2003). With a history of more than 2000 years, agriculture in the Yellow River basin is possibly an important reason for the observed high TAlk (Chen et al., 2005). Further, significant decreases in pH in the middle and lower Yellow River basin have been widely detected and are hypothesized to result from acid rain that is likely caused by anthropogenic sulfur emissions to the atmosphere (Guo et al., 2010). The reduced pH may have been partially responsible

for the elevated pCO_2 in these regions relative to the headwater region that had higher pH (Fig. 2).

Differences in the hydrochemical parameters between historical records and recent sampling clearly reveal the temporal changes over the period. Significant increase in pH at Toudaoguai was largely caused by widespread salinization of agricultural soils. There are two large irrigation zones upstream of Toudaoguai; large quantities of water is diverted for desalination and irrigation (Chen et al., 2005). The diverted water volume has gradually increased since 1960 due to growing demand (Ran et al., 2014). When washed out from irrigated farmlands, the return water characterized by high pH caused the riverine pH to increase, leading further to greatly reduced pCO_2 despite the roughly stable TAlk (Fig. 3b). Particularly, it is worth noting that the magnitude of reduction was much higher in the wet season when the high-pH return water reached the mainstem with floods (Table 2).

Trapping of water and suspended solids by dams will alter river-borne carbon dynamics (Cole et al., 2007). Extended residence time combined with sufficient organic matter availability may enhance CO_2 production, causing a higher pCO_2. This is particularly true for tropical reservoirs into which organic matter inputs are sufficient, especially in the initial years after impoundment (Roland et al., 2010; Raymond et al., 2013). On the other hand, reduced flow turbulence and increases in water residence time would promote photosynthesis of aquatic plants and reduce aqueous CO_2 concentration (Teodoru et al., 2009; Wang et al., 2011). An example of the impact of dams on downstream pCO_2 changes is presented in Fig. 8. Located on the upper mainstem channel (Fig. 1), operation of the Qingtongxia Dam since 1968 has substantially affected the pCO_2. Despite insignificant changes of the TAlk between the pre- and post-dam periods (Fig. 8), enhanced aquatic photosynthesis after dam operation owing to reduced TSS concentration may have absorbed aqueous CO_2 and resulted in increased pH by shifting the chemical equilibrium of Eq. (1). Accordingly, the riverine pCO_2 declined during the post-dam period with the elevated pH and roughly stable TAlk.

For the dams on the Loess Plateau constructed mostly in 1960–2000, however, aqueous photosynthesis appears to be at a low level owing to its extremely high TSS concentration and limited light availability (Chen et al., 2005). In contrast, flow regulation plays a more important role in controlling the seasonal patterns of downstream pCO_2. Man-made floods have been regularly released from the Xiaolangdi Dam sluice gates since 2000 to flush sediment deposition in the lower Yellow River, usually from late June (Wang et al., 2012; Ran et al., 2014). The deep waters supersaturated with CO_2 are first discharged, resulting in the high pCO_2 at Lijin in the wet season (Fig. 4c). Unlike the seasonal variations at Toudaoguai and Tongguan as mentioned above, duration of the high pCO_2 at Lijin coincided well with the sediment flushing period, indicating the impact of flow reg-

ulation on pCO_2 dynamics. Operation of dam cascade has also modified the TAlk and pCO_2 levels at the inter-annual scale. Affected by upstream dams (see Fig. 1), both the TAlk and pCO_2 at Lijin in the wet season were elevated during the period 2011–2012, by 22 and 20 %, respectively, relative to the baseline period 1950s–1984 (Table 2). Furthermore, soil conservation and vegetation restoration conducted on the Loess Plateau since the 1970s have contributed to the inter-annual changes. More organic carbon has been sequestrated as a result of these land management practices (Chen et al., 2007). Given the strong flushing and leaching effects of high-intensity rainfalls, riverine organic matter export tends to increase in the wet season, and the accompanying decomposition can elevate pCO_2.

4.3 Implications for CO_2 outgassing

CO_2 outgassing from river waters into the atmosphere during the carbon transport processes from land to the ocean has not been fully realized until recent years (Richey et al., 2002; Cole et al., 2007; Battin et al., 2009). Because riverine pCO_2 demonstrates the CO_2 concentration in surface water, a higher riverine pCO_2 usually represents stronger CO_2 outgassing under favourable environmental conditions, forming a carbon source for the atmosphere. However, accurate estimates of global CO_2 outgassing have been hampered by the absence of a spatially resolved pCO_2 database. Previous estimates from rivers alone involve large uncertainties, varying from 0.23 to 0.56 Gt C yr^{-1} (Cole et al., 2007; Aufdenkampe et al., 2011). A recent study has even concluded that up to 1.8 Gt of carbon is annually emitted from global rivers (Raymond et al., 2013), considerably higher than was previously thought. This estimate accounts for about 32 % of the annual carbon flux transferred from terrestrial systems to inland waters (Wehrli, 2013). Given the existing uncertainties, quantifying pCO_2 in different orders of streams of a complete river network is critical to resolve a robust estimate of riverine CO_2 evasion.

With respect to the Yellow River, the lower riverine pCO_2 in the HR sub-basin relative to the atmospheric equilibrium indicates a potential CO_2 drawdown. In comparison, the river waters in the remaining watershed are generally supersaturated with CO_2, mostly greater than 1000 µatm (Fig. 2b). With an average pCO_2 of 2810 ± 1985 µatm for the whole watershed comparable to the median of global rivers (i.e. 1300–4300 µatm; Aufdenkampe et al., 2011), the Yellow River waters tend to act as a net carbon source for the atmosphere. As stated earlier, despite the uncertainties associated with outgassing calculation, recent studies on watershed-scale carbon delivery demonstrate that CO_2 efflux from rivers can substantially exceed lateral carbon export (Richey et al., 2002). The Yellow River has experienced abrupt reductions in flow and TSS fluxes over the past decades and these reductions will continue in future. Its carbon fluxes reaching the ocean will therefore further decrease, and more carbon

is likely to be emitted as CO$_2$ into the atmosphere. In view of the severe soil erosion and high TSS transport (Syvitski et al., 2005), interpretation of these fluxes in the context of climate change is of great importance for understanding the role of Yellow River in the global carbon cycle.

5 Conclusions

The Yellow River was characterized by high alkalinity with a mean TAlk of 3665 ± 988 µmol L^{-1}. Although with significant spatial variations, the TAlk remained largely stable over the study period. However, it showed seasonal variability and decreased in the wet season, suggesting the dilution effect of water discharge. Except for the HR sub-basin where the pCO$_2$ was lower than the atmospheric equilibrium, river waters in the remaining watershed were supersaturated with CO$_2$. The basin-wide mean pCO$_2$ was estimated at 2810 ± 1985 µatm. Similar to the pH and TAlk, the pCO$_2$ also presented significant spatial and seasonal variations. The middle reaches, mainly the Loess Plateau, showed higher pCO$_2$ than the upper and lower reaches, which were principally resulting from severe soil erosion and the unique hydrological regime. The pCO$_2$ correlated exponentially with TSS transport when the erosion intensity was low and only the topsoils rich in organic carbon were eroded. When the TSS concentration exceeded 100 kg m^{-3} indicating the predominance of gully erosion, the subsoils with low organic carbon content were mobilized. Owing to the reduced organic carbon available for decomposition, the pCO$_2$ slightly decreased and remained stable thereafter, regardless of the increasing TSS concentration.

The observed spatial and temporal variations of riverine pCO$_2$ were collectively controlled by natural processes and human activities. High pCO$_2$ in the upper and middle reaches was usually estimated from March through May when ice-melt floods transported the accumulated CO$_2$-laden waters in winter. Human activities, especially flow regulation, have significantly changed its seasonal patterns by altering hydrological regime and riverine carbon delivery processes. While reduced turbidity and extended residence time due to dam trapping has enhanced aquatic photosynthesis and resulted in a decreased pCO$_2$, man-made floods through flow regulation would increase downstream pCO$_2$. Other anthropogenic perturbations, such as acidification, soil conservation and irrigation, have also affected pCO$_2$. The accelerating human activity within the watershed is likely to expand the role of anthropogenic over natural factors on the pCO$_2$ dynamics, because stronger anthropogenic impacts are certain to occur concerning present economic development. Considerably high riverine pCO$_2$ in the Yellow River waters with respect to the overlying atmosphere indicates that substantial amounts of CO$_2$ are emitted into the atmosphere. Given the huge human impacts on flow, TSS and carbon

fluxes, future efforts to estimate CO$_2$ evasion and assess its importance in the global carbon cycle are urgently needed.

References

Abril, G., Bouillon, S., Darchambeau, F., Teodoru, C. R., Marwick, T. R., Tamooh, F., Ochieng Omengo, F., Geeraert, N., Deirmendjian, L., Polsenaere, P., and Borges, A. V.: Technical Note: Large overestimation of pCO$_2$ calculated from pH and alkalinity in acidic, organic-rich freshwaters, Biogeosciences, 12, 67–78, doi:10.5194/bg-12-67-2015, 2015.

Alekin, O. A., Semenov, A. D., and Skopintsev, B. A.: Handbook of Chemical Analysis of Land Waters, Gidrometeoizdat, St. Petersburg, Russia, 269 pp., 1973.

Alin, S. R., Rasera, M. d. F. F. L., Salimon, C. I., Richey, J. E., Holtgrieve, G. W., Krusche, A. V., and Snidvongs, A.: Physical controls on carbon dioxide transfer velocity and flux in low-gradient river systems and implications for regional carbon budgets, J. Geophys. Res., 116, G01009, doi:10.1029/2010jg001398, 2011.

American Public Health Association (APHA): Standard Methods for the Examination of Water and Wastewater, 16th edition, American Public Health Association, Washington, DC, 1268 pp., 1985.

Aufdenkampe, A. K., Mayorga, E., Raymond, P. A., Melack, J. M., Doney, S. C., Alin, S. R., Aalto, R. E., and Yoo, K.: Riverine coupling of biogeochemical cycles between land, oceans, and atmosphere, Front. Ecol. Environ., 9, 53–60, 2011.

Battin, T. J., Luyssaert, S., Kaplan, L. A., Aufdenkampe, A. K., Richter, A., and Tranvik, L. J.: The boundless carbon cycle, Nat. Geosci., 2, 598–600, 2009.

Benstead, J. P. and Leigh, D. S.: An expanded role for river networks, Nat. Geosci., 5, 678–679, 2012.

Butman, D. and Raymond, P. A.: Significant efflux of carbon dioxide from streams and rivers in the United States, Nat. Geosci., 4, 839–842, 2011.

Chen, L. D., Gong, J., Fu, B. J., Huang, Z. L., Huang, Y. L., and Gui, L. D.: Effect of land use conversion on soil organic carbon sequestration in the loess hilly area, loess plateau of China, Ecol. Res., 22, 641–648, 2007.

Chen, S. and Ji, H.: Fuzzy optimization neural network approach for ice forecast in the Inner Mongolia Reach of the Yellow River, Hydrolog. Sci. J., 50, 319–330, 2005.

Chen, J., Wang, F. Y., Xia, X. H., and Zhang, L. T.: Major element chemistry of the Changjiang (Yangtze River), Chem. Geol., 187, 231–255, 2002a.

Chen, J., Tang, C. T., Sakura, Y., Kondoh, A., and Shen, Y.: Groundwater flow and geochemistry in the lower reaches of the Yellow River: a case study in Shandang Province, China, Hydrogeol. J., 10, 587–599, 2002b.

Chen, J., Wang, F., Meybeck, M., He, D., Xia, X., and Zhang, L.: Spatial and temporal analysis of water chemistry records (1958–2000) in the Huanghe (Yellow River) basin, Global Biogeochem. Cy., 19, GB3016, doi:10.1029/2004gb002325, 2005.

Clark, I. D. and Fritz, P.: Environmental isotopes in hydrogeology, CRC Press/Lewis Publishers, New York, 328 pp., 1997.

Clow, D. W. and Drever, J. I.: Weathering rates as a function of flow through an alpine soil, Chem. Geol., 132, 131–141, 1996.

Cole, J. J. and Caraco, N. F.: Atmospheric exchange of carbon dioxide in a low-wind oligotrophic lake measured by the addition of SF_6, Limnol. Oceanogr., 43, 647–656, 1998.

Cole, J. J., Prairie, Y. T., Caraco, N. F., McDowell, W. H., Tranvik, L. J., Striegl, R. G., Duarte, C. M., Kortelainen, P., Downing, J. A., Middelburg, J. J., and Melack, J.: Plumbing the global carbon cycle: Integrating inland waters into the terrestrial carbon budget, Ecosystems, 10, 171–184, 2007.

Epron, D., Farque, L., Lucot, E., and Badot, P. M.: Soil CO_2 efflux in a beech forest: dependence on soil temperature and soil water content, Ann. For. Sci., 56, 221–226, 1999.

Evans, W., Hales, B., and Strutton, P. G.: pCO_2 distributions and air-water CO_2 fluxes in the Columbia River estuary, Estuar. Coastal Shelf S., 117, 260–272, 2013.

Gaillardet, J., Dupre, B., Louvat, P., and Allegre, C. J.: Global silicate weathering and CO_2 consumption rates deduced from the chemistry of large rivers, Chem. Geol., 159, 3–30, 1999.

Guo, J. H., Liu, X. J., Zhang, Y., Shen, J. L., Han, W. X., Zhang, W. F., Christie, P., Goulding, K. W. T., Vitousek, P. M., and Zhang, F. S.: Significant acidification in major Chinese croplands, Science, 327, 1008–1010, 2010.

Hope, D., Palmer, S. M., Billett, M. F., and Dawson, J. J. C.: Variations in dissolved CO_2 and CH_4 in a first-order stream and catchment: an investigation of soil-stream linkages, Hydrol. Process., 18, 3255–3275, 2004.

Humborg, C., Mörth, C., Sundbom, M., Borg, H., Blenckner, T., Giesler, R., and Ittekkot, V.: CO_2 supersaturation along the aquatic conduit in Swedish watersheds as constrained by terrestrial respiration, aquatic respiration and weathering, Glob. Change Biol., 16, 1966–1978, 2010.

Hunt, C. W., Salisbury, J. E., and Vandemark, D.: Contribution of non-carbonate anions to total alkalinity and overestimation of pCO_2 in New England and New Brunswick rivers, Biogeosciences, 8, 3069–3076, doi:10.5194/bg-8-3069-2011, 2011.

Kato, T., Tang, Y., Gu, S., Cui, X., Hirota, M., Du, M., Li, Y., Zhao, X., and Oikawa, T.: Carbon dioxide exchange between the atmosphere and an alpine meadow ecosystem on the Qinghai-Tibetan Plateau, China, Agr. Forest Meteorol., 124, 121–134, 2004.

Lewis, E. and Wallace, D. W. R.: Program developed for CO_2 system calculations, ORNL/CDIAC-105, Carbon dioxide Information Analysis Center, Oak Ridge National Laboratory, Oak Ridge, TN, 1998.

Li, S., Lu, X. X., He, M., Zhou, Y., Li, L., and Ziegler, A. D.: Daily CO_2 partial pressure and CO_2 outgassing in the upper Yangtze

River basin: A case study of the Longchuan River, China, J. Hydrol., 466–467, 141–150, 2012.

Li, X. D., Fu, H., Guo, D., Li, X. D., and Wan, C. G.: Partitioning soil respiration and assessing the carbon balance in a *Setaria italica* (L.) Beauv. Cropland on the Loess Plateau, Northern China, Soil Biol. Biochem., 42, 337–346, 2010.

Liu, Q. and Singh, V.: Effect of microtopography, slope length and gradient, and vegetative cover on overland flow through simulation, J. Hydrol. Eng., 9, 375–382, 2004.

Melack, J.: Riverine carbon dioxide release, Nat. Geosci., 4, 821–822, 2011.

Millot, R., Gaillardet, J., Dupre, B., and Allegre, C. J.: The global control of silicate weathering rates and the coupling with physical erosion: new insights from rivers of the Canadian Shield, Earth Planet. Sci. Lett., 196, 83–98, 2002.

Piňol, J. and Avila, A.: Streamwater pH, alkalinity, pCO_2 and discharge relationships in some forested Mediterranean catchments, J. Hydrol., 131, 205–225, 1992.

Ran, L. and Lu, X. X.: Delineation of reservoirs using remote sensing and their storage estimate: an example of the Yellow River basin, China, Hydrol. Process., 26, 1215–1229, 2012.

Ran, L., Lu, X. X., Sun, H., Han, J., Li, R., and Zhang, J.: Spatial and seasonal variability of organic carbon transport in the Yellow River, China, J. Hydrol., 498, 76–88, 2013.

Ran, L., Lu, X. X., and Xin, Z.: Erosion-induced massive organic carbon burial and carbon emission in the Yellow River basin, China, Biogeosciences, 11, 945–959, doi:10.5194/bg-11-945-2014, 2014.

Raymond, P. A. and Cole, J. J.: Increase in the export of alkalinity from North America's largest river, Science, 301, 88–91, 2003.

Raymond, P. A., Hartmann, J., Lauerwald, R., Sobek, S., McDonald, C., Hoover, M., Butman, D., Striegl, R., Mayorga, E., and Humborg, C.: Global carbon dioxide emissions from inland waters, Nature, 503, 355–359, 2013.

Richey, J. E., Melack, J. M., Aufdenkampe, A. K., Ballester, V. M., and Hess, L. L.: Outgassing from Amazonian rivers and wetlands as a large tropical source of atmospheric CO_2, Nature, 416, 617–620, 2002.

Roland, F., Vidal, L. O., Pacheco, F. S., Barros, N. O., Assireu, A., Ometto, J. P., Cimbleris, A. C., and Cole, J. J.: Variability of carbon dioxide flux from tropical (Cerrado) hydroelectric reservoirs, Aquat. Sci., 72, 283–293, 2010.

Rustomji, P., Zhang, X., Hairsine, P., Zhang, L., and Zhao, J.: River sediment load and concentration responses to changes in hydrology and catchment management in the Loess Plateau region of China, Water Resour. Res., 44, W00A04, doi:10.1029/2007WR006656, 2008.

Shi, W.-Y., Tateno, R., Zhang, J.-G., Wang, Y.-L., Yamanaka, N., and Du, S.: Response of soil respiration to precipitation during the dry season in two typical forest stands in the forest-grassland transition zone of the Loess Plateau, Agr. Forest Meteorol., 151, 854–863, 2011.

Striegl, R. G., Dornblaser, M., McDonald, C., Rover, J., and Stets, E.: Carbon dioxide and methane emissions from the Yukon River system, Global Biogeochem. Cy., 26, GB0E05, doi:10.1029/2012GB004306, 2012.

Syvitski, J. P. M., Vorosmarty, C. J., Kettner, A. J., and Green, P.: Impact of humans on the flux of terrestrial sediment to the global coastal ocean, Science, 308, 376–380, 2005.

Teodoru, C. R., del Giorgio, P. A., Prairie, Y. T., and Camire, M.: Patterns in pCO$_2$ in boreal streams and rivers of northern Quebec, Canada, Global Biogeochem. Cy., 23, GB2012 doi:10.1029/2008gb003404, 2009.

Tranvik, L. J., Downing, J. A., Cotner, J. B., Loiselle, S. A., Striegl, R. G., Ballatore, T. J., Dillon, P., Finlay, K., Fortino, K., Knoll, L. B., Kortelainen, P. L., Kutser, T., Larsen, S., Laurion, I., Leech, D. M., McCallister, S. L., McKnight, D. M., Melack, J. M., Overholt, E., Porter, J. A., Prairie, Y., Renwick, W. H., Roland, F., Sherman, B. S., Schindler, D. W., Sobek, S., Tremblay, A., Vanni, M. J., Verschoor, A. M., von Wachenfeldt, E., and Weyhenmeyer, G. A.: Lakes and reservoirs as regulators of carbon cycling and climate, Limnol. Oceanogr., 54, 2298–2314, 2009.

Wallin, M. B., Grabs, T., Buffam, I., Laudon, H., Ågren, A., Öquist, M. G., and Bishop, K.: Evasion of CO$_2$ from streams–The dominant component of the carbon export through the aquatic conduit in a boreal landscape, Glob. Change Biol., 19, 785–797, 2013.

Wang, F. S., Wang, B. L., Liu, C. Q., Wang, Y. C., Guan, J., Liu, X. L., and Yu, Y. X.: Carbon dioxide emission from surface water in cascade reservoirs-river system on the Maotiao River, southwest of China, Atmos. Environ., 45, 3827–3834, 2011.

Wang, X., Ma, H., Li, R., Song, Z., and Wu, J.: Seasonal fluxes and source variation of organic carbon transported by two major Chinese Rivers: The Yellow River and Changjiang (Yangtze) River, Global Biogeochem. Cy., 26, GB2025, doi:10.1029/2011gb004130, 2012.

Wang, Z., Liu, G., and Xu, M.: Effect of revegetation on soil organic carbon concentration in deep soil layers in the hilly Loess Plateau of China, Acta Ecologica Sinica, 30, 3947–3952, 2010 (in Chinese).

Wehrli, B.: Biogeochemistry: Conduits of the carbon cycle, Nature, 503, 346–347, 2013.

Wu, L. L., Huh, Y., Qin, J. H., Du, G., and van der Lee, S.: Chemical weathering in the Upper Huang He (Yellow River) draining the eastern Qinghai-Tibet Plateau, Geochimi. Cosmochim. Ac., 69, 5279–5294, 2005.

Wu, W., Xu, S., Yang, J., and Yin, H.: Silicate weathering and CO$_2$ consumption deduced from the seven Chinese rivers originating in the Qinghai-Tibet Plateau, Chem. Geol., 249, 307–320, 2008.

Xu, J.: Implication of relationships among suspended sediment size, water discharge and suspended sediment concentration: the Yellow River basin, China, CATENA, 49, 289–307, 2002.

Yao, G. R., Gao, Q. Z., Wang, Z. G., Huang, X. K., He, T., Zhang, Y. L., Jiao, S. L., and Ding, J.: Dynamics of CO$_2$ partial pressure and CO$_2$ outgassing in the lower reaches of the Xijiang River, a subtropical monsoon river in China, Sci. Total Environ., 376, 255–266, 2007.

Zhang, J., Huang, W. W., Létolle, R., and Jusserand, C.: Major element chemistry of the Huanghe (Yellow River), China: Weathering processes and chemical fluxes, J. Hydrol., 168, 173–203, 1995.

Zhang, J., Xu, M., Wang, Z., Ma, X., and Qiu, Y.: Effects of revegetation on organic carbon storage in deep soils in hilly Loess Plateau region of Northwest China, Chinese Journal of Applied Ecology, 23, 2721–2727, 2012 (in Chinese).

Zhao, M. X., Zhou, J. B., and Kalbitz, K.: Carbon mineralization and properties of water-extractable organic carbon in soils of the south Loess Plateau in China, Eur. J. Soil Biol., 44, 158–165, 2008.

Zhao, W.: The Yellow River's Sediment, Yellow River Conservancy Press, Zhengzhou, China, 807 pp., 1996.